



**HAL**  
open science

## NUCLEAR STRUCTURE AT HIGH SPINS

F.S. Stephens

► **To cite this version:**

F.S. Stephens. NUCLEAR STRUCTURE AT HIGH SPINS. Journal de Physique Colloques, 1980, 41 (C10), pp.C10-1-C10-8. 10.1051/jphyscol:19801001 . jpa-00220620

**HAL Id: jpa-00220620**

**<https://hal.science/jpa-00220620>**

Submitted on 4 Feb 2008

**HAL** is a multi-disciplinary open access archive for the deposit and dissemination of scientific research documents, whether they are published or not. The documents may come from teaching and research institutions in France or abroad, or from public or private research centers.

L'archive ouverte pluridisciplinaire **HAL**, est destinée au dépôt et à la diffusion de documents scientifiques de niveau recherche, publiés ou non, émanant des établissements d'enseignement et de recherche français ou étrangers, des laboratoires publics ou privés.

## NUCLEAR STRUCTURE AT HIGH SPINS\*

F.S. Stephens.

*Nuclear Science Division, Lawrence Berkeley Laboratory, University of California, Berkeley, CA 94720, U.S.A.*

Abstract.- Nuclear structure at the highest spins is very likely to involve both collective and single-particle aspects. The liquid-drop model favors shapes that imply combinations of collective (rotational) and rotation-aligned single-particle angular momenta. The detailed band structures for the full range of such mixtures are considered.

Nuclei are composed of a small (but not too small) number of nucleons. As a result they display both collective and single-particle (non-collective) features. For example, in the rare-earth and actinide regions, the low-lying rotational bands represent an almost pure collective motion, with energies following the  $I(I + 1)$  rotor formula to within a percent or two, and E2 transition probabilities nearly 200 times larger than a single proton would have. On the other hand, near the closed shells, the energy levels are almost completely determined by the motion of a single nucleon. Most nuclear levels display both collective and non-collective features, and high-spin states are no exception. To approach the physics of these states I will first describe some properties of a purely collective, classical rotor, and then consider the effects of coupling single particle motion to this. The objective is to understand the kinds of mixtures of collective and single particle motion that are important in nuclei at the highest spins. Our ideas about such

states have undergone important developments recently that now make possible a reasonably simple description of this subject, which I will try to present.

All nuclei seem to have some collective features at the highest spins. The collective limit is thus one we must understand, and the basic nuclear system here has been found to be an axially symmetric rotor with quadrupole deformation. The moment of inertia of a classical rotor depends on both the shape and the flow pattern, the latter of which is expected to be rigid in nuclei at high spins. The pairing correlations modify this significantly at low spins values, but are expected to be completely quenched by spins of  $30\hbar$  or so. The shape of a rigid ellipsoid can be expressed in terms of the parameters,  $\sigma$  and  $\gamma$ , defined so that the semi-axes  $r_i$  are related to the mean radius  $R$  by;  $r_i = a_i R$ , where:

$$\begin{aligned} a_1 &= e^{\sigma} \cos(\gamma - 2\pi/3) \\ a_2 &= e^{\sigma} \cos(\gamma + 2\pi/3) \\ a_3 &= e^{\sigma} \cos\gamma \end{aligned} \quad (1)$$

For small deformation this gives  $\Delta R/R \approx \epsilon \approx 1.5\sigma$  and  $\beta \approx 1.6\sigma$ . Such an ellipsoid has moment of inertia:

\* Presented at the International Conference on Nuclear Behavior at High Angular Momentum, Strasbourg, France, April 22-24, 1980.

$$\begin{aligned} \mathcal{J}_1 &= \frac{1}{5} M (r_2^2 + r_3^2) \\ &= \frac{1}{2} (a_2^2 + a_3^2) \mathcal{J}_0 \end{aligned} \quad (2)$$

where  $\mathcal{J}_0$  is the rigid sphere value, and the axes may be permuted cyclically. Values of  $\mathcal{J}_0$  can be obtained from the expression for a rigid sphere given by Myers<sup>1</sup>. From the equivalent sharp radius for the matter distribution:<sup>2</sup>

$$R_s = 1.28 A^{1/3} - 0.76 + 0.8 A^{-1/3} \text{ fm} ; \quad (3)$$

the value for a sphere is:

$$\frac{2\mathcal{J}_0}{\hbar^2} = \frac{4MR_s^2}{5\hbar^2} = 0.01913 A R_s^2 (\text{fm}) \text{ MeV}^{-1} . \quad (4)$$

The effect of a diffuse surface can be added simply by:

$$\mathcal{J}_{\text{diff}} = \mathcal{J}_{\text{sharp}} + 2 Mb^2 , \quad (5)$$

where b is the width of the diffuse region, normally around 1 fm. For orientation one can use the simpler expression:

$$R = 1.16 A^{1/3} \text{ fm} , \quad (6)$$

which leads to:

$$\hbar^2/2\mathcal{J}_0 = 36 A^{-5/3} \text{ MeV} . \quad (7)$$

The general behavior of the moments of inertia of rigid ellipsoids, as given by eqn. 2, is shown in Fig. 1. These are for prolate, P, or oblate,

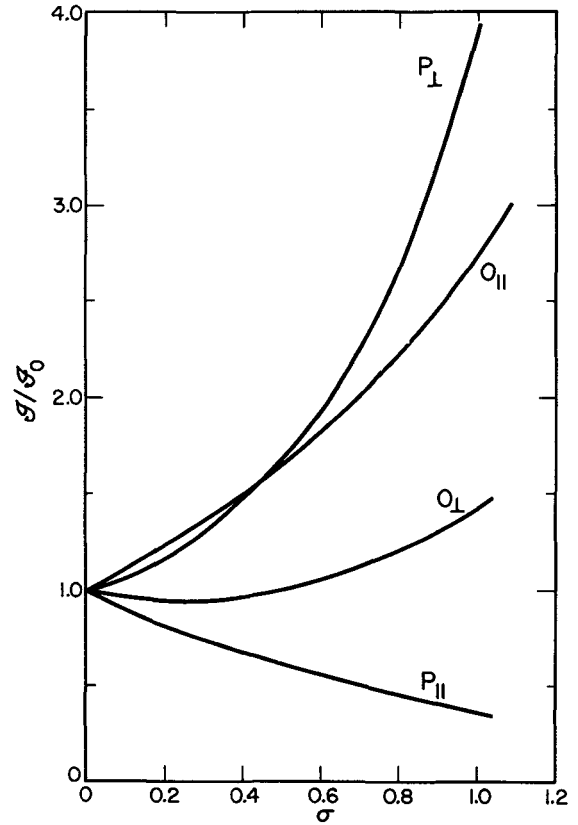


Fig. 1. Rigid-body moments of inertia for the appropriate shapes and axes as a function of the deformation parameter,  $\sigma$  (eqn. (1)).

O, shapes rotating about the symmetry axis,  $\parallel$ , or about an axis perpendicular to it,  $\perp$ . For rigid-flow behavior, triaxial shapes will fall between these limits. The oblate shape rotating about its symmetry axis and the prolate shape rotating about a perpendicular axis clearly have the largest moments of inertia and thus the lowest rotational energies. These two configurations have similar values for reasonable deformations ( $\sigma \gtrsim 0.6$ ), and, in fact, cross around  $\sigma = 0.5$ . It is not, a priori, apparent that the full liquid-drop energy will follow this behavior since there is also a shape dependence in both the surface and Coulomb energies. However, when the deformation is expressed in terms of  $\sigma$  (eqn. 1), the shape ( $\gamma$ ) dependence of the surface and Coulomb energies comes in only as a high-order term (third order

in  $\sigma$ ), so that the full liquid-drop energy at high spins does follow rather closely the moment-of-inertia behavior shown in Fig. 1. The crossing from oblate to prolate shape, as lowest in energy, comes just prior to fission in the full liquid-drop treatment, around  $\sigma = 0.5$ . The point of this discussion is that the macroscopic liquid-drop behavior of nuclei favors two particular situations,  $P_{\perp}$  and  $O_{\parallel}$  (and the triaxial pathway between these), and the questions of interest are: (1) is this energy gain significant; and (2) if so, what kind of microscopic nuclear structure is implied.

The lowest order expansions of eqn. 2 for the situations shown in Fig. 1 are illustrated in Fig. 2. These expansions begin to deviate significantly from the exact expressions around  $\beta = 0.3$  ( $\sigma = 0.2$ ), as can be seen in Fig. 1. The energy trajectories based on these four cases of classical rigid rotation for  $\beta = 0.3$  are shown in the right part of Fig. 2. The lowest energies are for an oblate shape rotating about the symmetry axis, corresponding to its largest moment of inertia. The earth is oblate for precisely this reason; however, real rotating nuclei are generally not oblate due to the shell effects, as will be discussed shortly.

For systems where the quantal aspects are important, the preceding discussion has to be clarified, since these systems cannot rotate collectively about a symmetry axis—there is no way to orient them with respect to such an axis. It was understood for some time that this meant these degrees of freedom were contained in the single-particle motion. However, when Bohr and Mottelson<sup>3</sup> considered aligning particle angular momentum along a symmetry axis, they realized that on the average the energy was the same as for rotating the system classically about that axis. They have strictly shown this only in the Fermi

gas approximation, but it is generally believed to be true, or approximately so, for realistic nuclear systems. Particle angular momenta aligned along a nuclear symmetry axis are then viewed as an effective rotation of the system about that axis. Thus the trajectories sketched in the right part of Fig. 2 all have meaning for nuclei; the solid ones are true collective rotations, having smooth energies and strongly enhanced E2 transition probabilities, whereas the dashed lines are the average location of irregularly spaced states having single-particle character. Both features of the latter-type states suggest that isomers should be reasonably probable, and these expectations have led to a number of searches for them, as will be discussed by other speakers.

To this picture the microscopic aspects of nuclear structure must be added. Nuclear levels in a potential well are grouped together into shells in very much the same way electrons are in an atom. Certain nucleon numbers ("magic numbers") complete shells and have extra stability in analogy to the noble gas electronic structures. However, when nuclei deform, the shells change, so that the number to complete a shell is different. Thus, in general, a given nucleon number will prefer that shape which makes it look most nearly like a closed shell. These "shell effects" can be as large as 10-12 MeV (the double closed spherical shell at  $^{208}\text{Pb}$ ), but on the average might be 3-4 MeV. Comparing with the right side of Fig. 2, it is apparent that 3-4 MeV is larger than the full spread of liquid-drop shapes up to  $I \approx 30$ . Thus below this spin (for  $A \sim 160$ ) the nuclear shape is determined mainly by shell effects. Around  $I = 60$ , however, the spread in Fig. 2 is  $\sim 10$  MeV, considerably larger than the normal shell effects, so that here one expects the liquid-drop effects to dominate, producing mainly oblate shapes rotating

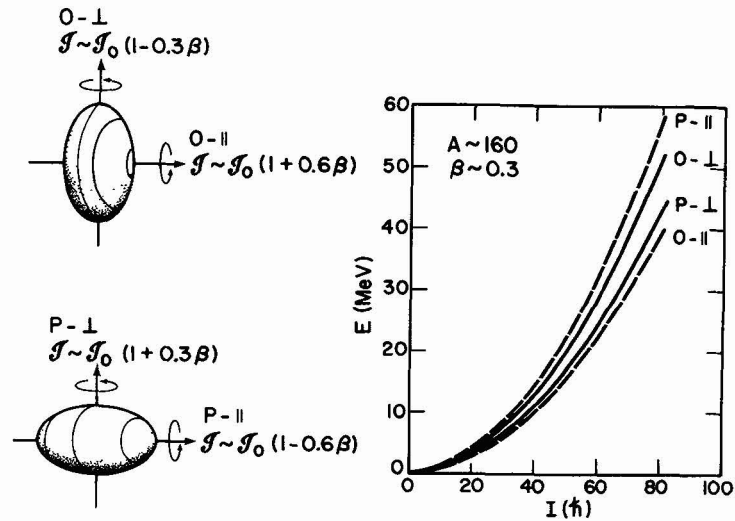


Fig. 2. The left side shows the lowest-order estimates for the rigid-body moments of inertia in terms of the deformation parameter,  $\beta$  ( $\approx 1.6\sigma$ ). The right side shows the corresponding energy trajectories for  $\beta = 0.3$  and mass number 160.

around the symmetry axis (non-collective behavior with isomers) or prolate shapes rotating collectively (smooth bands and no isomers), or some intermediate triaxial configurations.

In order to understand how single particle and collective motion might be combined in nuclear states at high spins, I will start with a collective rotational nucleus, and couple to this first one and then more single particles. The rotational angular momentum is necessarily perpendicular to the nuclear symmetry axis (as discussed above) and the particle angular momentum,  $j$ , can couple either along the symmetry axis as illustrated in the top part of Fig. 3, or along the rotation axis as in the bottom part of Fig. 3. The former situation is that considered by Bohr<sup>4</sup> and the projection of  $j$  along the symmetry axis, called  $\Omega$ , is a constant of the motion. In this case the collective angular momentum,  $R$ , and the projection of  $j$  along the rotation axis are not constants of the motion. In the lower part of Fig. 3, the projection of  $j$  along the rotation axis, called  $\alpha$  (or  $i$ ), is sharp, and here  $R$  and  $\Omega$  are not

constants of the motion. It seems rather clear that a perpendicular relationship between  $R$  and  $j$  will be much less favorable for producing low-energy high-spin states than a parallel one. This is borne out by the fact that as the nucleus rotates there is a Coriolis force which tends to align  $j$  with the rotation axis. The back-bending phenomenon, and a number of other related effects, are now known to be connected with such "rotation-aligned" states. In the remainder of this lecture I want to try to trace how the inclusion of such states can effect a smooth transition between fully collective and fully non-collective regions of nuclear behavior.

In the upper left portion of Fig. 4 a complete collective behavior is illustrated. The nucleus is taken to be prolate, as indicated by the small  $\beta, \gamma$  plot, and each intrinsic state (angular momentum along the symmetry axis is ignored, implying  $K = 0$ ) has a collective rotational band corresponding to rotation about the axis perpendicular to the symmetry axis. The total angular momentum is just that of the collective motion,  $\omega\epsilon$ . In

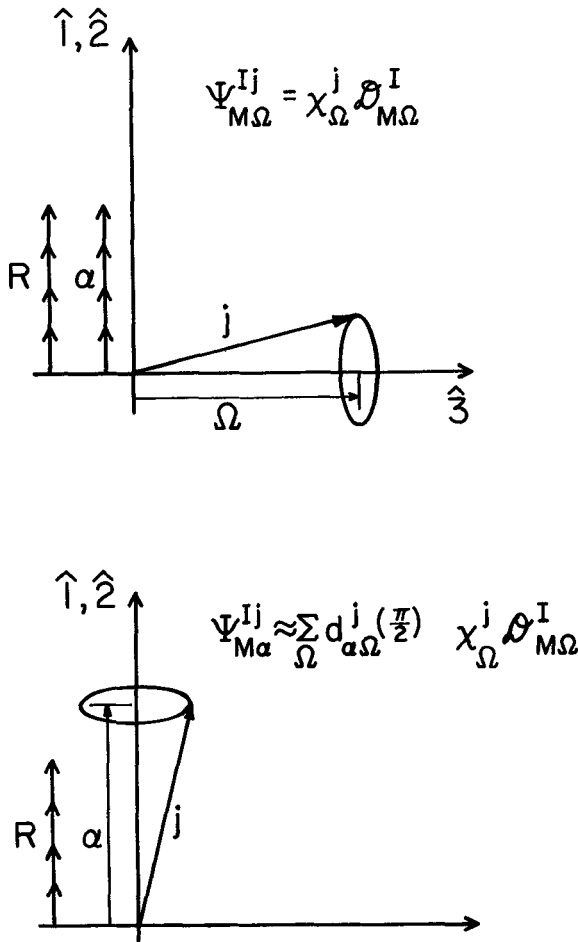


Fig. 3. Schematic vector diagrams illustrating the deformation-aligned coupling scheme (above) and the rotation-aligned coupling scheme (below). The  $\hat{3}$  axis is the nuclear symmetry axis and the vertical axis is taken to be the rotation axis, located in the  $\hat{1}, \hat{2}$  plane.

such bands the energy is given by

$$E(I) = R^2/2\theta + E_0 \approx I^2/2\theta + E_0 \quad (8)$$

where  $\theta = \mathcal{J}/\hbar^2$ ,  $E_0$  is a band-head energy, and one is neglected compared with  $I$ . These are just parabolas centered on the  $y$ -axis and displaced vertically by  $E_0$ . The  $\gamma$ -ray energy in such a band is related to the slope of this parabola:

$$E(I) = 2 \frac{dE(I)}{dI} \Big|_{\theta} = \frac{4I}{2\theta} \quad (9)$$

where  $\theta$  is assumed to remain constant. The difference between successive  $\gamma$ -ray energies is related to the curvature of the parabolas:

$$\begin{aligned} \Delta E_{\gamma}(I) &= 2 \frac{dE_{\gamma}(I)}{dI} \Big|_{\theta} \\ &= 4 \frac{d^2E(I)}{dI^2} \Big|_{\theta} = \frac{8}{2\theta} \end{aligned} \quad (10)$$

and is independent of spin for a perfect rotor ( $\theta$  constant).

In the upper right portion of Fig. 4 a small amount of single particle angular momentum aligned along the rotation axis,  $j_a$ , has been added. The orbits of these particles are roughly in the plane perpendicular to the rotation axis, and will cause a bulge in the otherwise prolate nucleus. Thus the nucleus necessarily becomes slightly tri-axial as indicated in the small  $\beta, \gamma$  plot. The total angular momentum is now the sum of the collective part,  $\omega_{coll}$ , and a single particle part,  $\Sigma j_a$ . The energy of the bands is given by:

$$\begin{aligned} E(I) &= R^2/2\theta_{coll} + E(j_a) = \\ &(I - j_a)^2/2\theta_{coll} + E(j_a) \quad (11) \end{aligned}$$

where  $E(j_a)$  is the band-head energy and  $\theta$  for the collective rotation is specifically labeled  $\theta_{coll}$ . These are parabolas whose horizontal displacement from the  $y$ -axis is  $j_a$  and whose vertical displacement is  $E(j_a)$ . The solid lines in Fig. 4 represent these bands. If one assumes  $j_a$  and  $\theta_{coll}$  to be fixed in each band, then the collective E2  $\gamma$ -ray energy is again just twice the slope of these bands and is given by:

$$E_{\gamma}(I) = 2 \frac{dE(I)}{dI} \Big|_{j_a, \theta_{coll}} = \frac{4(I - j_a)}{2\theta_{coll}} \quad (12)$$

The assumption of constant  $j_a$  and  $\theta_{coll}$ , need not be valid, since these quantities could change

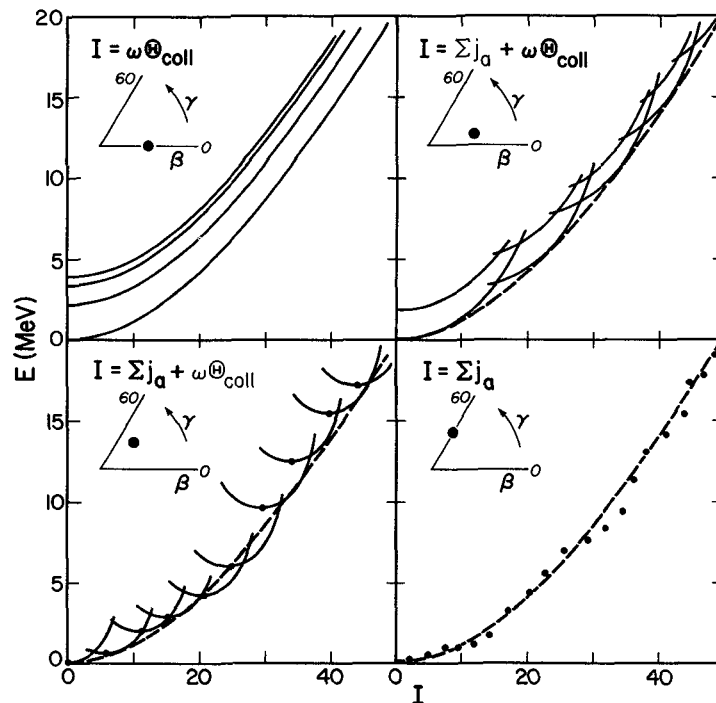


Fig. 4. Schematic excitation energy vs spin plots for various relative amounts of collective angular momentum and single-particle rotation-aligned angular momentum. Bandhead (pure single-particle) energies are shown in the lower two panels. The solid curves correspond to real bands, whereas the dashed curve is the envelope of the real bands.

gradually within a given band, however there are now both experimental and theoretical reasons to believe this is a reasonable assumption. The normal form for writing eqn. (12) was given as eqn. (9); and since the aligned angular momentum,  $j_a$ , is not usually known, one generally just uses eqn. (9), and  $\theta$  becomes an "effective" value,  $\theta_{eff}$ , defined by this relationship. There is no displacement,  $j_a$ , in eqn. (9), so that it corresponds to the envelope curve (dashed) in Fig. 4. The average slope, and thus  $E_Y(I)$ , are the same for this envelope and for the populated portion (near the envelope) of the real bands, so that one cannot distinguish the real band structure this way. From the  $\gamma$ -ray energies, one gets only the properties of the envelope, which are the appropriate values to compare with those for the rigid classical rotors discussed in connection with

Figs. 1 and 2. The fact that there is aligned angular momentum inevitably reduces the collective (band) moment of inertia, as a given particle cannot contribute fully to both the alignment and the moment of inertia. Thus the curvature of the real bands in the upper right part of Fig. 4 is larger than that of the envelope. This curvature is still related to differences between  $\gamma$ -ray energies:

$$\begin{aligned} \Delta E_Y(I) &= 2 \left. \frac{dE_Y(I)}{dI} \right|_{j_a, \theta_{coll}} \\ &= 4 \left. \frac{d^2 E(I)}{dI^2} \right|_{j_a, \theta_{coll}} = 8/\theta_{coll} \end{aligned} \quad (13)$$

Note that this difference is sensitive to  $\theta_{coll}$ , but must be between two (correlated)  $\gamma$ -rays within

the same band, and cannot be a difference of average  $\gamma$ -ray energies. There are now experiments sensitive to this curvature,<sup>5,6</sup> and Bent Herskind will discuss them tomorrow. The pattern illustrated in this portion of Fig. 4 has considerable experimental support. The sketched band crossings correspond to backbends, the first of which in the yrast sequence is very well studied, and the second in this sequence has been seen in several cases. In a few nuclei, as many as four or five backbends have been observed in bands above the yrast line. This behavior will be discussed by R. Bengtsson and others this afternoon. It is clear that rotational nuclei generally behave this way.

In the lower left part of Fig. 4, the alignment process is assumed to continue. The nucleus is moving toward an oblate shape as more particles align and thereby move in roughly circular orbits perpendicular to the rotation axis. The total angular momentum is now mostly aligned,  $\Sigma j_a$ , with only a modest collective contribution. The band head energies are indicated as dots, and they have moved out rather close to the envelope line. As sketched (somewhat arbitrarily), there is only an average of 6 or  $8\hbar$  in the bands at the spins where they are likely to be populated (along the envelope). The band heads were not indicated in the previous panel (upper right) where they were rather far from the envelope line--15-20 $\hbar$  on the average--corresponding to a considerably larger collective contribution to the total angular momentum. The curvature of the bands is much larger now since the shape is becoming more oblate, and the rotation axis will then become a symmetry axis. Another way to view this is that most of the reasonably high- $j$  particles are aligned and thus no longer contribute to the collective moment of inertia. These bands show a much higher rate of crossing, and although the slope ( $e_{eff}$ ) behaves regularly,

the detailed band structure will be quite irregular. It is worth emphasizing that the  $\gamma$ -ray energies alone cannot distinguish among these first three panels; one must look at the  $\gamma$ -ray energy correlations.

Finally in the lower right part of Fig. 4 the nucleus has acquired an axially symmetric oblate shape--the rotation axis has become the symmetry axis and collective rotations cannot exist about this axis. The band heads now scatter around the envelope line and are purely single-particle states. At  $\beta = 0$  these would be the usual spherical shell-model states, but reasonably large  $\beta$  values may also occur. Such states are observed in several regions and will be discussed later by Khoo and others. We have thus followed the motion from collective to non-collective in a continuous way by aligning more and more particles.

Several comments about this transition should be made. First the general pattern as more angular momentum is added would be to progress through the panels aligning more and more particles. However, this can be altered at any point by shell effects, just as the starting prolate shape is due to a shell effect. Furthermore, at some high spin the liquid drop model suggests that the nuclear structure will be dominated by shapes with very large prolate deformations--prior to fission. These will produce a "bending over" of the envelope curve and probably a shift to less alignment. A number of us are hunting for this "giant" backbend. Finally, in the last panel, and perhaps the next-to-last one, there can be important collective rotations about the perpendicular axis, provided  $\beta$  is not too small. At high spins the bands corresponding to this rotation rise rather steeply off the yrast line, and it is not clear what role they will play. In the lower left panel, these combine with the bands shown to give the

well known behavior of a triaxial rotor. One could expect M1 transitions from such bands when the amount of collective angular momentum is small, and the presence of two types of E2 transitions might tend to smear out the regular rotational behavior.

This sequence of events is not the only one possible. There can be prolate nuclei rotating about their symmetry axis (band heads in the first panel) or, the collective rotation of oblate nuclei (mentioned briefly above). However, the sequence discussed traces out the situations favored by the liquid drop model. One expects these to be the most common, if not the only, combinations of collective and non-collective motion at high spins. Furthermore there is good evidence that nuclei do exist with behavior like that shown in the first, second, and fourth panels. I believe we now have the experimental tools to

determine whether nuclei at the very highest spins fall into this sequence, and if so, where. The next few years should thus be exciting ones in the study of very high-spin states.

#### References

1. Myers, W. D. 1973. Nucl. Phys. A204:465.
2. Blocki, J., Randrup, J., Swiatecki, W. J., Tsang, C. F. 1976. Ann. Phys. 105:427.
3. Bohr, A. and Mottelson, B. R. 1975. Nuclear Structure. Vol. 2. Reading, Mass: Benjamin.
4. Bohr, A. 1952. Mat. Fys. Medd. Dan. Vid. Selsk. 26: No. 14.
5. Andersen, O., Garrett, J. D., Hagemann, G. B., Herskind, B., Hillis, D. L., Riedinger, L. L. 1979. Phys. Rev. Lett. 43:687.
6. Deleplanque, M. A., Stephens, F. S., Andersen, O., Ellegaard, C., Garrett, J. D., Herskind, B., Fossan, D., Neiman, M., Roulet, C., Hillis, D. C., Kluge, H., Diamond, R. M., Simon, R. S. 1980. Phys. Rev. Lett. In press.